# RESIDUAL DEFORMATION REDUCTION AND STRENGTH IMPROVEMENT IN COMPOSITE T-JOINT USING ASYMMETRIC LAMINATE DESIGN AND ATYPICAL DELTOID STRUCTURE

S. Hisada[1], K. Takagaki[2], S. Minakuchi[3], and N. Takeda[4]

[1] Department of Advanced Energy, Graduate School of Frontier Sciences, The University of Tokyo, 5-1-5 Kashiwanoha, Kashiwa, Chiba, 277-8561, Japan
Email: hisada@smart.k.u-tokyo.ac.jp
Web page: http://www.smart.k.u-tokyo.ac.jp/official/english/index_en.html

**Keywords:** T-joint, Asymmetric lamination, Deltoid, Fiber orientation

## ABSTRACT

One of the difficulties in composite structural application is joining components. A T-joint is one of the important elements in aircraft structures that transfers load between vertical and horizontal panels. In composite T-joints, process induced residual deformation such as spring-in occurs due to anisotropy of material properties. This deformation leads to residual stress during assembly and causes premature failure. Moreover, T-joints often fail at low load in the curved region of the L-shaped parts or deltoid area because of its low through-thickness strength properties and process-induced defects.

Previous works mainly focused on mechanical properties on T-joints under tensile or bending load, not considering the effect of residual deformation caused in the manufacturing process. In this current study, we applied the asymmetric lamination to the whole L-shaped parts in a T-joint specimen to suppress spring-in deformation. We evaluated the effectiveness of the proposed design using a three-dimensional shape measurement system. It was revealed that spring-in deformation can be reduced without extra deformation in the planar parts using the proposed asymmetric laminate design.

The deltoid region is also an important factor for T-joint's fracture. The fracture of deltoid often leads to final failure. In previous work, the effect of deltoid geometries and material properties on the T-joint's failure behavior was studied. However, deltoid structure such as fiber orientation was not considered. In this current research, we proposed new deltoid structure, which has looped fibers in the deltoid region, to improve the strength of T-joint components. We conducted tensile tests while measuring cross-sectional strain distribution using digital image correlation (DIC). We used asymmetric laminate design, fiber-looped deltoid, and hybrid structure that combined them. All types of the specimens showed improvement in initial failure load and maximum load compared to the conventional ones, confirming the effectiveness of the proposed design.

## 1 INTRODUCTION

A T-joint is a typical joining component used in aircraft structures. The basic design of T-joint is illustrated in Figure 1. It is composed of two L-shaped parts, skin, and deltoid filling in the space. T-joint takes on an important role as a medium of vertical and horizontal panels to transfer load. Composite T-joint has been shown to fail mostly in deltoid and corner regions of L-shaped parts. The problem is that premature failure often occurs due to low through-thickness material properties and inevitable cure-induced defects. Process-induced shape distortion is another problem that reduces T-joint's strength. When manufacturing composite parts with complex shape, shape distortion occurs especially in the radius region (i.e., spring-in deformation) due to the difference between in-plane and out-of-plane thermal and cure shrinkage strains (Figure 2). Correcting the distorted geometry into the original shape causes residual stress, which results in the reduced strength.

Previous works mainly aimed at understanding fracture characteristic of T-joints under tensile or bending loading both numerically and experimentally. Burns et al. studied the effect of stacking sequence on tensile property [1, 2]. However, few works considered the influence of cure-induced residual deformation. Meanwhile some studies addressed deltoid's geometry and material properties to

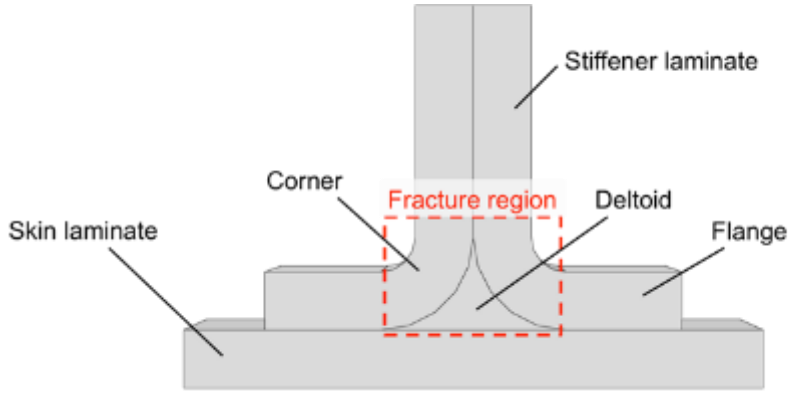


Figure 1. Typical T-joint showing main components.

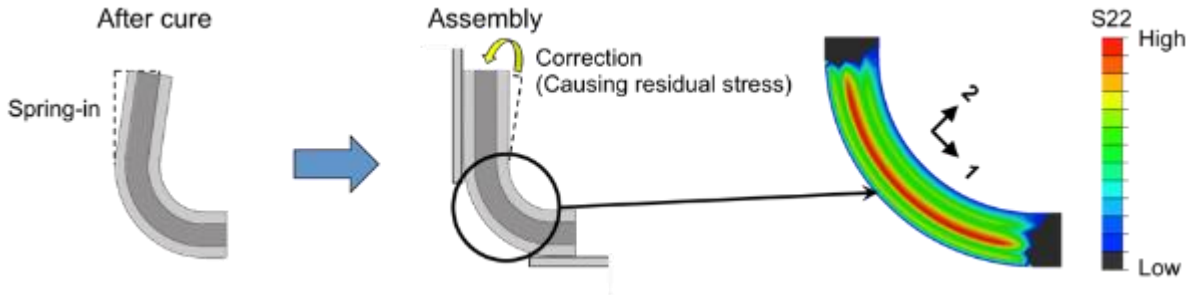


Figure 2. Residual stress caused by correcting spring-in deformation.

enhance strength of parts [3-6]. Trask et al. investigated the influence of process-induced defects in deltoid on the failure of composite T-joints [7]. Nevertheless, the effect of deltoid configuration such as fiber orientation has not been studied.

In this current study, we propose asymmetric laminate design for reducing residual deformation and validate through three-dimensional shape measurements. We also propose an atypical deltoid structure for improving strength of T-joint and verify the effectiveness by tensile tests and strain measurements using digital image correlation (DIC).

## 2 RESIDUAL DEFORMATION REDUCTION USING ASYMMETRIC LAMINATE

### 2.1 Asymmetric laminate

Asymmetric laminate composites exhibit large distortion in the out-of-plane direction after cure. It is mainly caused by bending-stretching coupling due to orthotropic material properties such as stiffness and coefficient of thermal expansion. This characteristic usually makes it difficult to apply asymmetric laminates to structural elements. However, Radford et al. proposed to reduce spring-in deformation in L-shaped part using asymmetric laminates [8]. In this previous work, asymmetric laminates were used only at the corner of L-shaped parts to suppress shape distortion in the flanges (Figure 3). This method was shown to be effective on reducing spring-in deformation in thin L-shaped parts. However, complex manufacturing process was necessary to change the stacking sequence only at the corner. Moreover, stress concentration might occur at discontinuous stacking region. Contrastively, in T-joints, the stacking sequence of whole stiffener becomes symmetric even if each L-shaped part is an asymmetric laminate (Figure 4). In addition, deformation in flange is restrained by the skin laminate. Therefore, spring-in deformation in T-joints can be reduced without distortion in the flanges and stress concentration.

In this section, we propose asymmetric laminate design to suppress residual deformation. The design is validated through three-dimensional shape measurement.

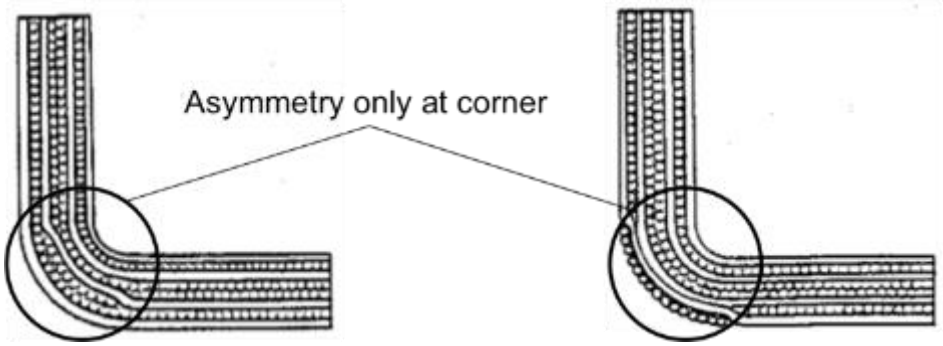


Figure 3. Design for reducing spring-in deformation in L-shaped composite proposed in [8].

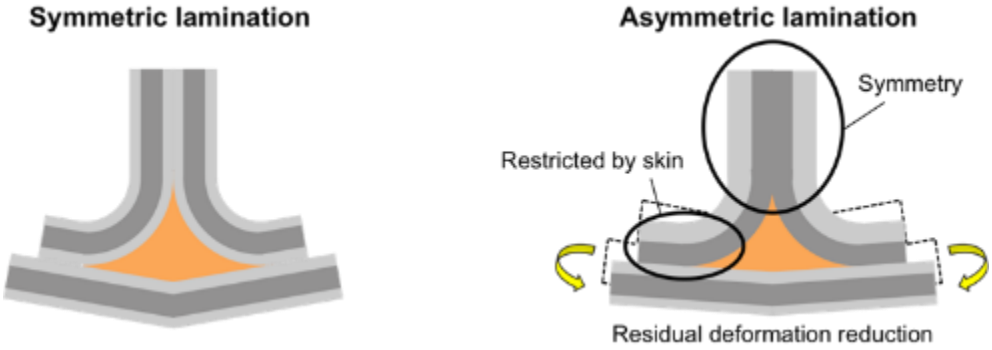


Figure 4. Design concept for reducing residual deformation without excess distortion proposed in this current study.

### 2.2 Experimental methods of three-dimensional shape measurement

Figure 5 shows the specimen's geometry and the definition of fiber direction. The T-joint has 80 mm high stiffener, and 200 mm long skin. Unidirectional carbon/epoxy prepreg sheets, T700S/2592 (Toray Industries, Inc.), were used in this study. Stacking sequence in L-shaped parts were [02/902]2S as a conventional symmetric laminate and [06/904/0/904/0] as an asymmetric laminate. The skin was laid up with the sequence of [02/902]2S in both specimens. The deltoid was filled with the same unidirectional prepreg sheets in 90º direction according to the volume of the space. Adhesive films (FM-300; Cytec Industries, Inc.) were inserted into each part interface. All parts were assembled and vacuum bagged (Figure 6). Specimens were cured in an autoclave at 130 ºC under 0.3 MPa.

Three-dimensional shape measurement was conducted for the two types of the specimens to validate the effectiveness of the proposed asymmetric laminate design. ATOS Core scanner (GOM Industries, Ltd.) was used in combination with ATOS Inspect software (Figure 7(a)). Markers were attached on the specimen surface as reference points and the specimen was sprayed for preventing degradation in measurements caused by halation (Figure 7(b)). Two specimens were prepared for each stacking sequence and tested.

### 2.3 Experimental results of three-dimensional shape measurement

Figure 8 shows the three-dimensional shape of each specimen. Spring-in deformation was calculated using the bottom surface of skin for avoiding the effect of thickness variation due to resin leakage and nonuniform pressurization. In the symmetric laminate, 0.81º spring-in deformation was generated. On the other hand, spring-in deformation was 0.60º in the proposed asymmetric laminate, showing 0.21º reduction. This result is attributed to 90º layers concentrated near the interface between the deltoid region and the L-shaped parts. The 90º layers shrink much more than the 0º layers, leading to in-plane compressive strain. This strain caused bending moment for spring-out and suppressed the spring-in deformation. Specimens used in this study were 100 mm long from the center to the edge, meaning that the difference of 0.37 mm out-of-plane displacement between the symmetric and asymmetric specimen

was come up in the edge. In practical large-scale structures, the displacement (i.e., gap between two mating components) further increases and significant stress can be induced after assembly.

Figure 9 represents the gauss-fitting plane of the stiffener and the flange in each specimen. Since the edges are usually trimmed off, the plane was fitted without 20 mm from the edges. In the flange, maximum deviation of out-of-plane displacement between the real plane and the fitting one was 0.054 mm in the symmetric laminate and 0.057 mm in the asymmetric one. In the stiffener, maximum deviation was 0.0072 mm in the symmetric one and 0.0084 mm in the asymmetric one, showing adequately small value. From these results, it was confirmed that spring-in deformation can be reduced without distortion in the flange and the stiffener.

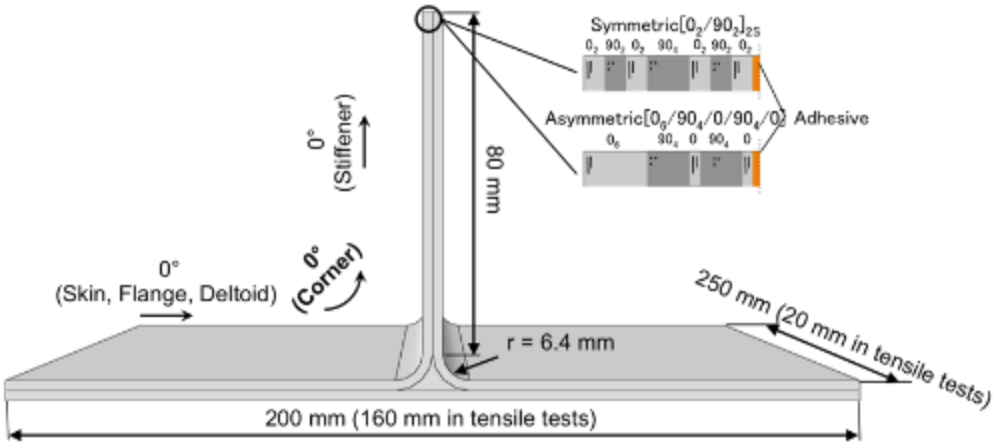


Figure 5. Schematic of specimen used in three-dimensional shape measurements and tensile tests.

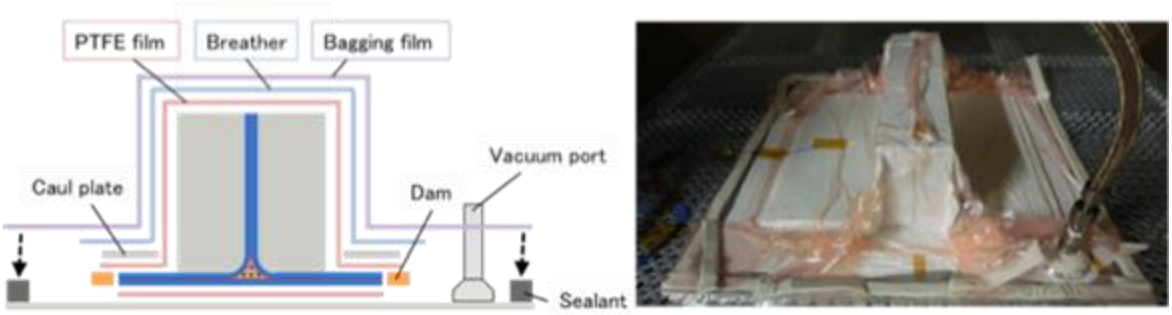


Figure 6. Schematic of vacuum-bagging assembly.

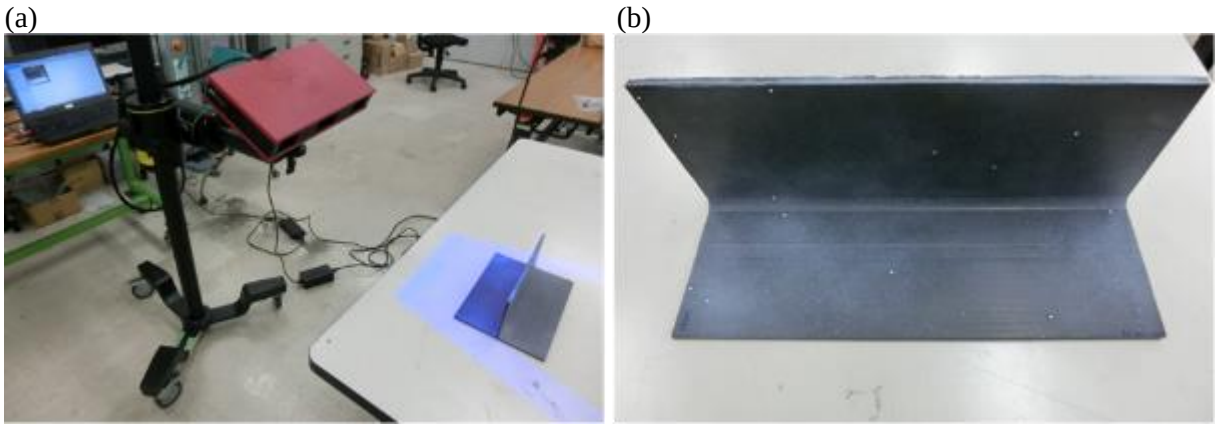


Figure 7. Schematic of three-dimensional shape measurement. (a) Setup. (b) Specimens.

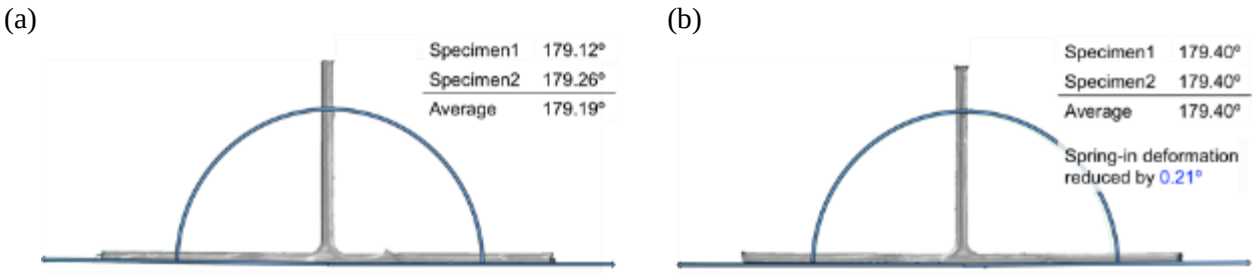


Figure 8. Spring-in deformation in (a) symmetric, (b) asymmetric laminate design.

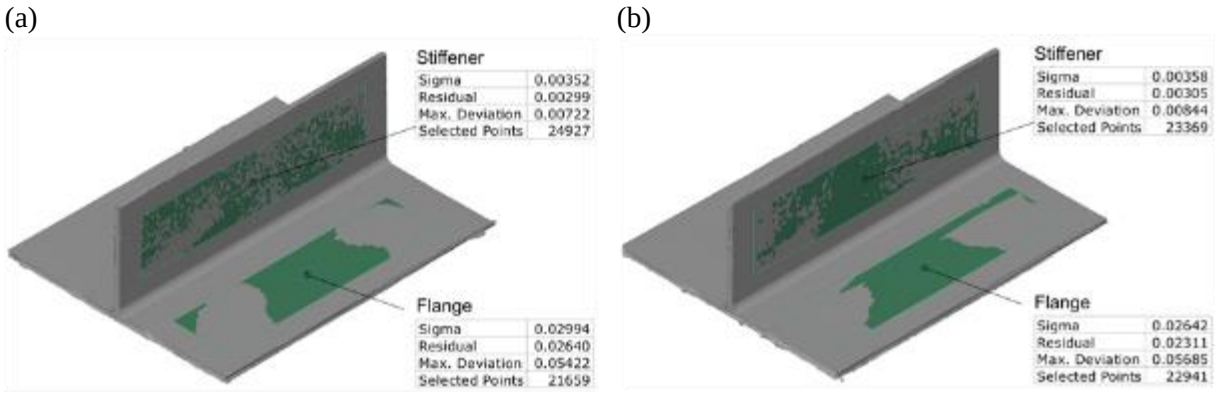


Figure 9. Deviation of plane of specimens in (a) symmetric, (b) asymmetric laminate design.

## 3 STRENGTH IMPROVEMENT USING ATYPICAL DELTOID STRUCTURE

### 3.1 Deltoid structure

In most cases, composite T-joint fails in deltoid and corner regions of L-shaped parts. Figure 10 shows the typical tensile failure behavior in T-joints with stacking sequence of [02/902]2S. Initial failure occurs along 6-7ply interface in the corner region. Then, crack propagates through the deltoid region and finally along the interface between the skin and the L-shaped parts. This failure is mainly attributed to lateral deformation in fracture region. Figure 11 represents the numerical result of the strain in the lateral direction under tensile load as seen in the global coordinate system. When the stiffener laminate is pulled up, fracture region deforms in the lateral direction due to the constraint of the 0° layers at the surface side and skin bending. This deformation causes out-of-plane stresses, especially out-of-plane shear stress, leading to T-joint's fracture. Therefore, restraint of lateral deformation in the fracture region is needed for strength improvement.

In this current study, we propose a new deltoid structure as referred to fiber-looped deltoid, which has looped fibers in the deltoid region (Figure 12). In this structure, fiber layers are added to the deltoid side of the L-shaped parts, leading to higher bending stiffness. Therefore, the lateral deformation can be suppressed by using this structure. In this section, we conduct tensile tests while measuring the cross-sectional strain change using digital image correlation (DIC) to validate the effectiveness of the proposed deltoid structure (Table 1). We also use the asymmetric laminate design in section 2 and hybrid structure, which combines fiber-looped deltoid and asymmetric lamination.

### 3.2 Experimental methods of tensile test

Four types of specimens were used in the tensile tests (Symmetric, Asymmetric, Fiber-looped, Hybrid, Table 1). Specimens with 20 mm width were cut out from the ones used in the three-dimensional shape measurements (Figure 5). The stiffener was clamped and pulled up at a rate of 1.0 mm per minute. DIC measurement was conducted during the tensile tests using ARAMIS 5M (GOM Industries, Ltd.) to measure the strain development.


Figure 10. Typical fracture behaviour in conventional T-joint.

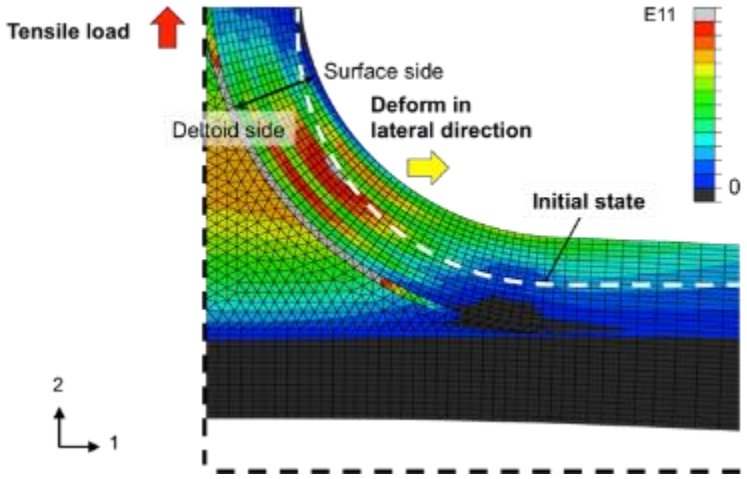


Figure 11. Lateral deformation under tensile load causing T-joint fracture.

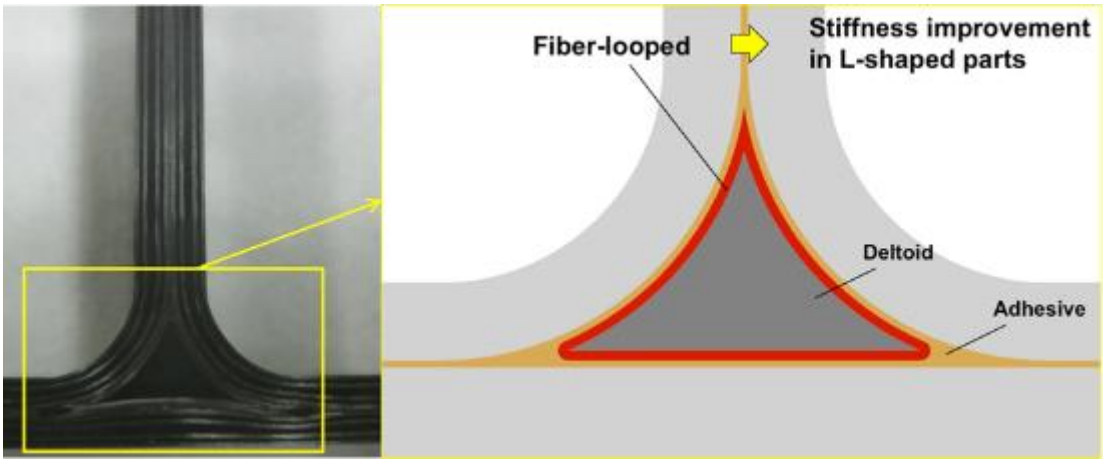


Figure 12. Schematic of fiber-looped deltoid structure.

| | Symmetric | Asymmetric | Fiber-looped | Hybrid |
|---|---|---|---|---|
| L-shaped part | $\mathbf{[0_2/90_2]_{2S}}$ | $\mathbf{[0_6/90_4/0/90_4/0]}$ | $\mathbf{[0_2/90_2]_{2S}}$ | $\mathbf{[0_6/90_4/0/90_4/0]}$ |
| Skin | $\mathbf{[0_2/90_2]_{2S}}$ | | | |
| Deltoid | 90º ply | 90º ply | Fiber loop + 90º ply (Figure 12) | Fiber loop + 90º ply |

Table 1. Specimens used in tensile tests.

### 3.3 Experimental results and discussions

Figure 13 shows initial failure load and displacement depending on the specimen configuration. The

points indicate the average values and the error bars represent the standard deviation. The symmetric specimen failed along 6-7ply interface at 2.86 kN (Figure 14 (a)). Other types of specimens also fractured at the same place. In the asymmetric specimen, failure load was 2.96 kN and improved by 3.3% compared to the symmetric one. It is attributed to the residual stress reduction. Figure 15 shows the residual out-of-plane normal stress when the spring-in deformation after cure is corrected. In the asymmetric laminate design, the stress was reduced by 5.0 MPa at the fracture point. Therefore, the reduction of the residual stress by the spring-in deformation suppression led to the improvement of initial failure strength. Fiber-looped deltoid specimens failed at 3.26 kN. It was 13.8% higher than the symmetric specimen. Figure 16 shows the lateral strain distribution under 2.6 kN tensile load obtained by DIC. In the fiber-looped deltoid, the strain was remarkably reduced compared to the symmetric specimen. From these results, it was confirmed that lateral deformation can be suppressed using fiber-looped deltoid, leading to strength improvement. In the hybrid structure, lateral strain was reduced in the same way as the fiber-looped deltoid. Failure load was 3.05 kN and improved by 6.6% compared to the symmetric laminate. However, it was weaker than the fiber-looped deltoid specimen. This may be attributed to the stress concentration arisen from the continuous 90º layers.

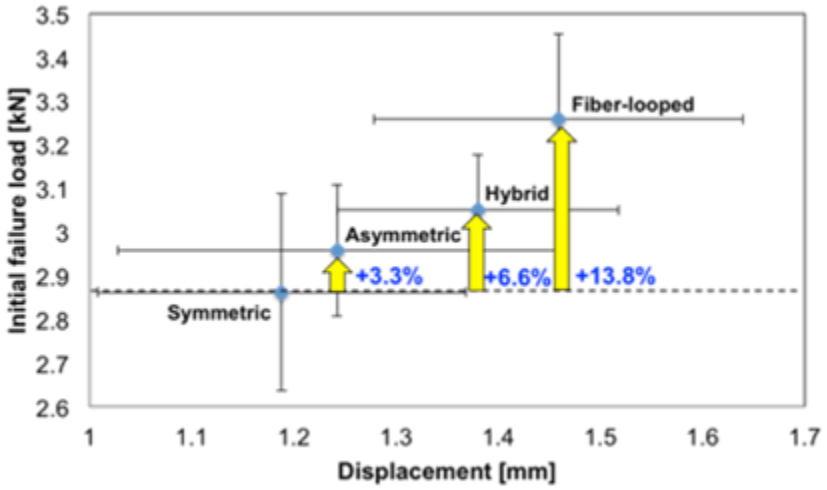


Figure 13. Initial failure load and displacement depending on specimen configuration.

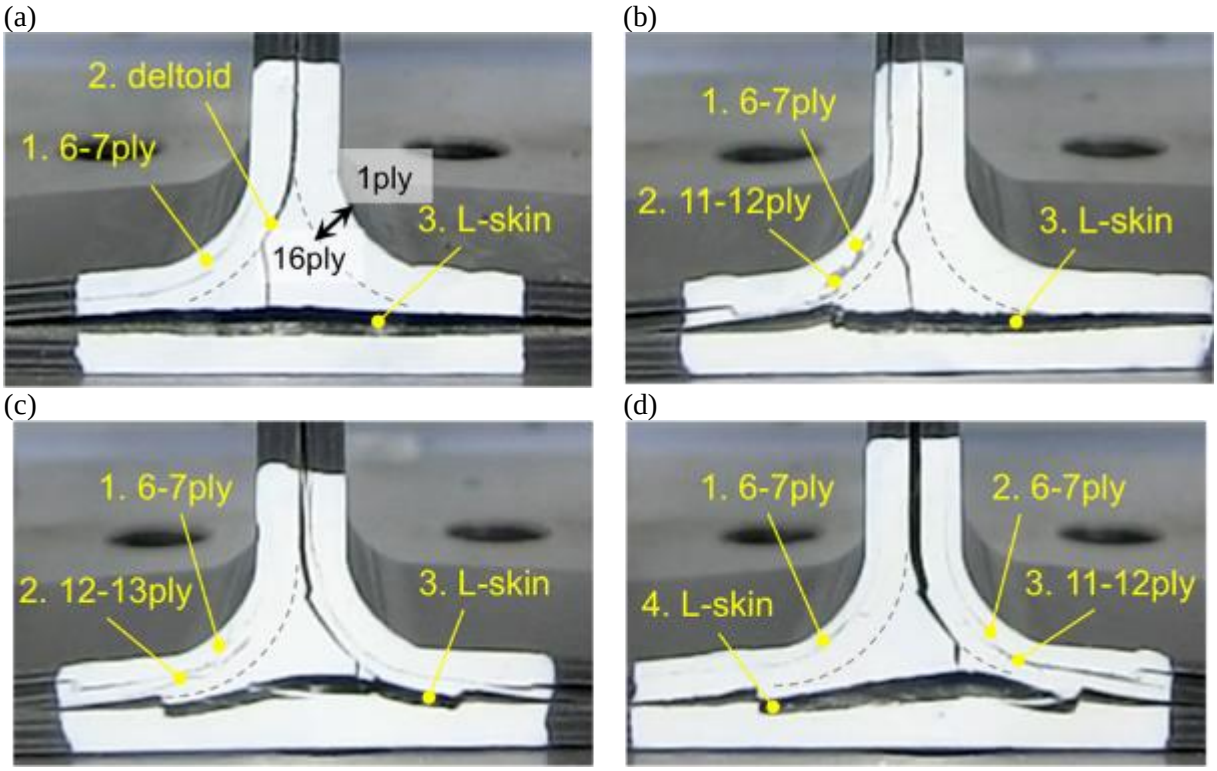


Figure 14. Cross sectional view of fracture. (a) Symmetric laminate design.
(b) Asymmetric laminate design. (b) Fiber-looped deltoid. (d) Hybrid Structure.

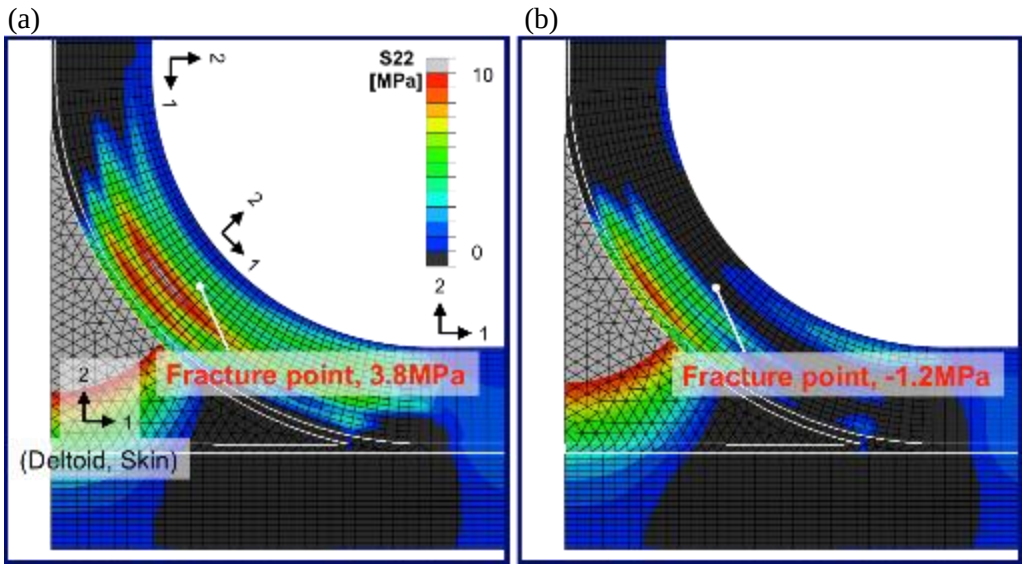


Figure 15. Residual out-of-plane normal stress when correcting spring-in deformation.
(a) Symmetric laminate design. (b) Asymmetric laminate design.

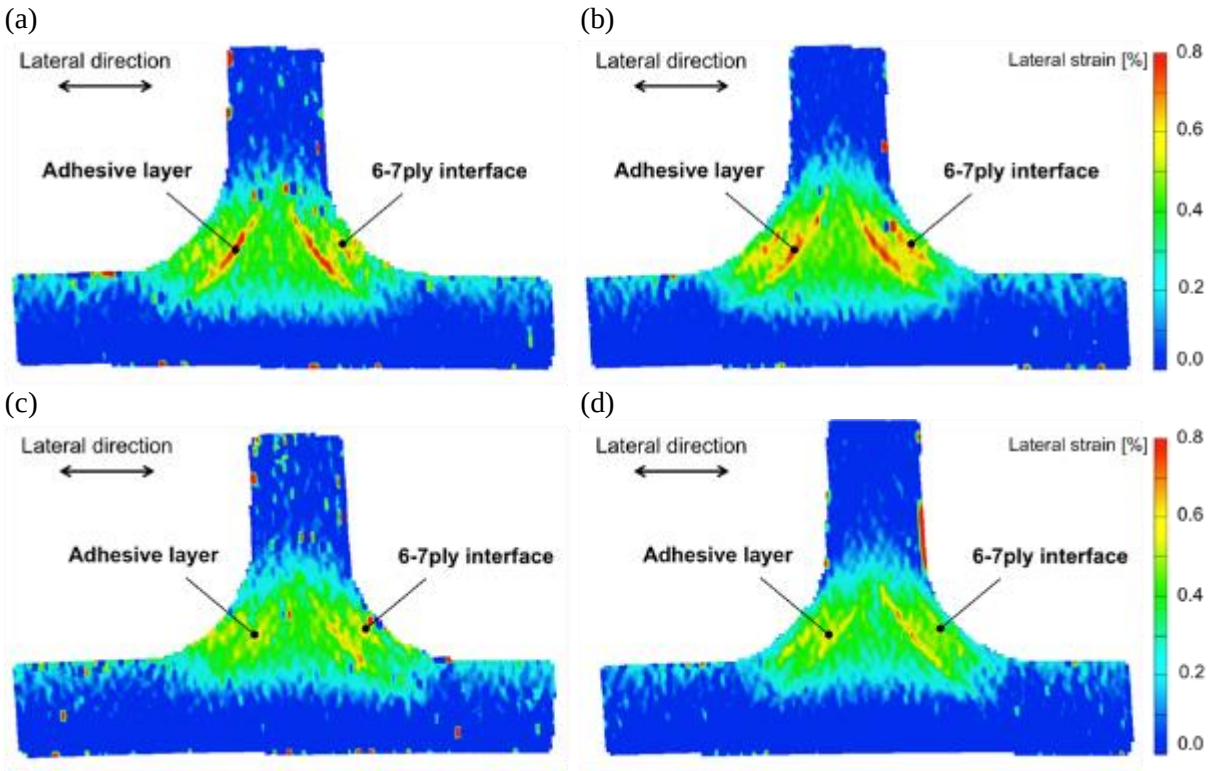


Figure 16. Lateral strain distribution obtained from DIC. (a) Symmetric laminate design. (b) Asymmetric laminate design. (c) Fiber-looped deltoid. (d) Hybrid structure.

Figure 17 shows maximum load and displacement at that point. The points indicate the average values and the error bars represent the standard deviation. The symmetric specimen failed just after the deltoid fracture and the maximum load was 3.27 kN. In the asymmetric specimen, the maximum load was 3.54 kN and improved by 8.3% compared to the symmetric one. In the fiber-looped deltoid, the maximum load of 3.56 kN was achieved, which was 9.2% higher than the symmetric one. In the hybrid structure, the maximum load was 4.08 kN and improved by 24.9% compared to the symmetric one.

The maximum load significantly increased from the initial load in the asymmetric laminate design and the hybrid structure. Figure 18 shows the distribution of out-of-plane shear stress calculated using the finite element analysis, which includes the initial cracks of each specimen. The analytical model was cooled down from 130 ºC to 20 ºC and pulled up with 3.0 kN. In the symmetric specimen, the crack tip reached the end of the corner of the L-shaped part. In contrast, the crack stopped at the middle of the corner in the asymmetric specimen. As a result, stress concentration occurred at the tip of the crack. Moreover, asymmetric laminate design has two places of four serial 90º layers (7-10ply, 12-15ply). In these layers, transverse cracks are easily generated across the layers. These two factors caused next failure at the 11-12ply interface and released the fracture energy. Therefore, asymmetric laminate was able to endure larger load than the symmetric one. In the hybrid structure, stress did not concentrate at the crack tip like the symmetric laminate design. Hence, second failure occurred at the 6-7ply interface in the other side or in the adhesive. Figure 19 shows the von-Mises stress in the adhesive. In the hybrid structure, von-Mises stress was reduced 4.4% compared to the symmetric one. Consequently, though second failure occurred in the adhesive, the hybrid structure failed at the 6-7ply interface in the other side of the initial failure. This crack induced third failure at 11-12ply interface. Hybrid structure released the energy in three places of four serial 90º layers, leading to significantly increase of maximum load. In summary, though continuous 90º layers had disadvantageous effect on initial failure load, maximum load was improved due to the energy release by the failure at these places.

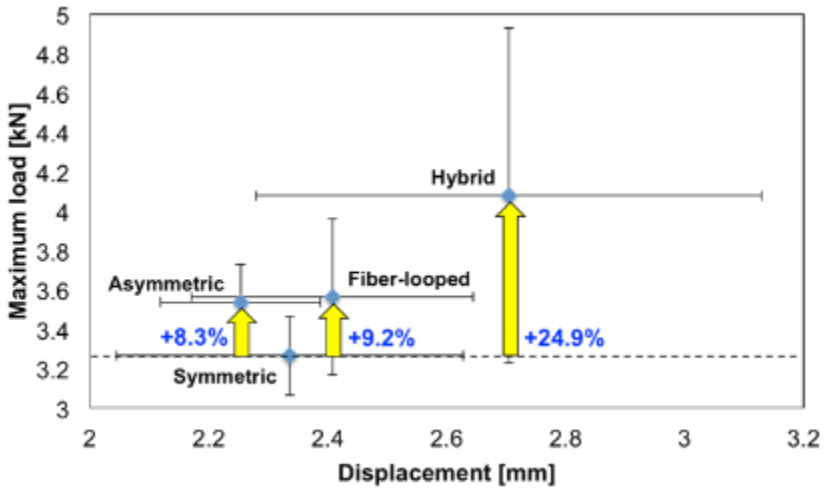


Figure 17. Maximum load and displacement at that point.

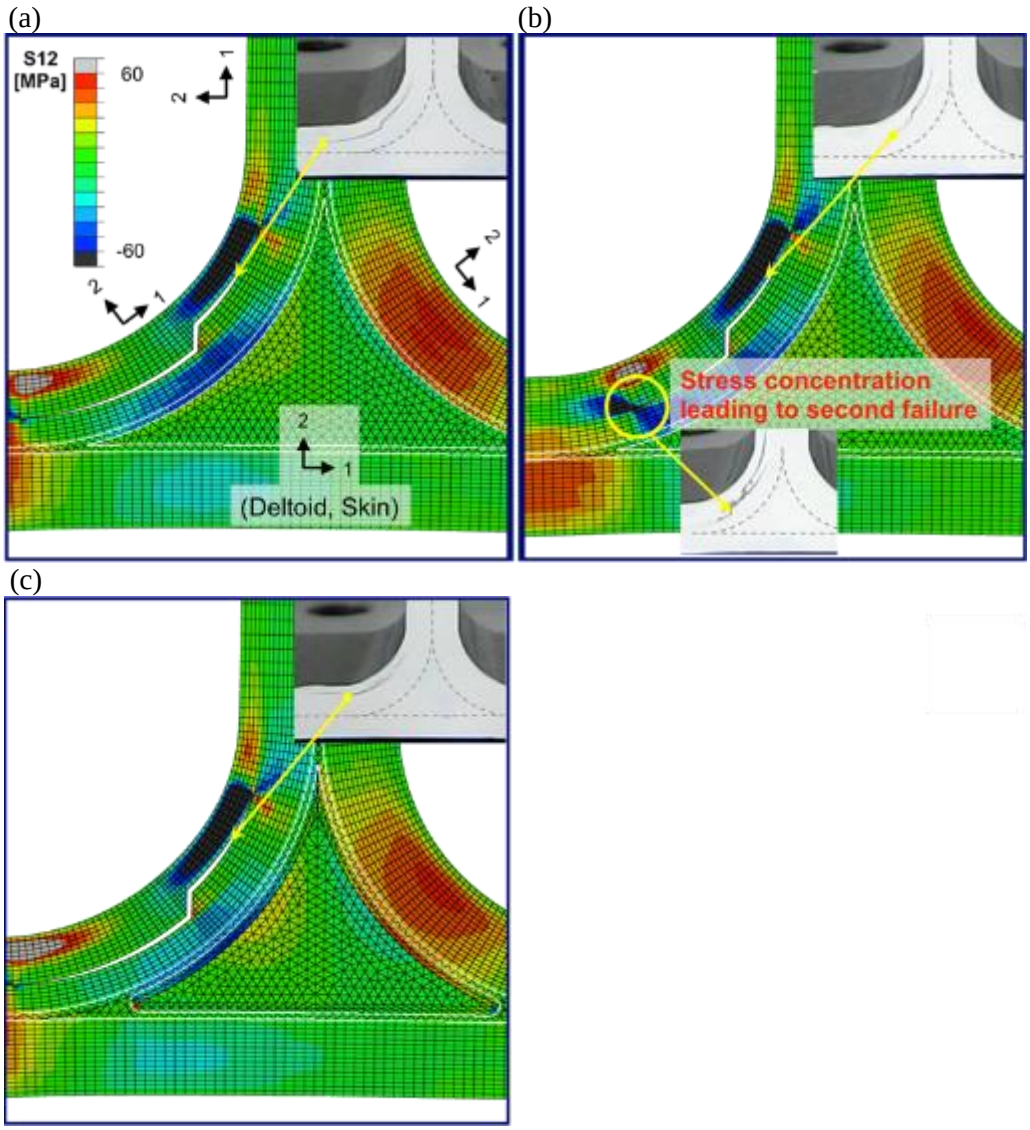


Figure 18. Out-of-plane shear stress distribution after the initial failure.
(a) Symmetric laminate design. (b) Asymmetric laminate design. (c) Hybrid structure.

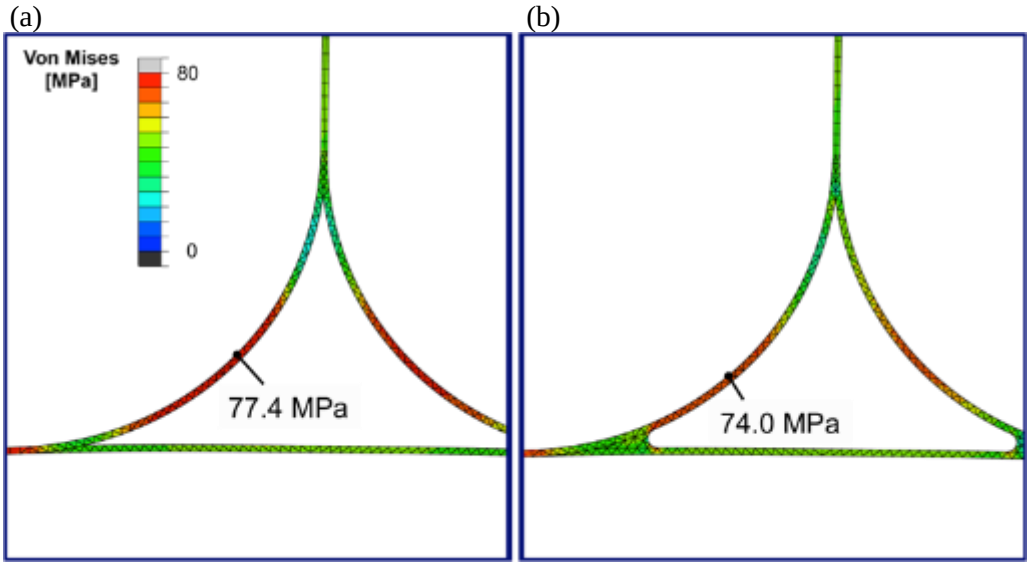


Figure 19. Von-Mises stress distribution in the adhesive.
(a) Symmetric laminate design. (b) Hybrid structure.

## 4 CONCLUSIONS

In this study, we proposed new T-joint's designs using asymmetric lamination and a fiber-looped deltoid structure. From the results of three-dimensional shape measurements, it was revealed that spring-in deformation could be reduced 0.21° without shape distortion in planar sections by applying the asymmetric lamination to L-shaped parts. In addition, initial failure load and maximum load were also enhanced compared to the symmetric laminate, showing that suppression of residual deformation leads to strength improvement. From the DIC tests, it was confirmed that lateral deformation was restrained by using the fiber-looped deltoid. As a result, initial failure load was improved by 13.8%, showing the effectiveness of the structure. Hybrid structure, which combines asymmetric lamination and fiber-looped deltoid, reduced spring-in deformation and enhanced both initial failure load and maximum load. Especially in maximum load, 24.9% improvement was achieved compared to the symmetric specimen.

This study used 16ply laminate in each part. However, thicker laminates are adopted in aircraft primary structures, leading to larger residual stress. Future work examines the effectiveness of the proposed designs in thicker laminates. Moreover, the design will be optimized changing the parameters of stacking sequence, the number of looped fiber, and so on.

## ACKNOWLEDGEMENTS

This research was funded by JSPS Grant-in-Aid for Scientific Research (S) Number 26220912. This paper was also partially supported by SIP (Cross-ministerial Strategic Innovation Promotion Program) – SM4I (Structural Materials for Innovation) by the Council for Science, Technology and Innovation (CSTI), Japan.

## REFERENCES

[1] L. Burns, A.P. Mouritz, D. Pook and S. Feih, Strengthening of composite T-joints using novel ply design approaches, *Composites Part B*, **88**, 2016, pp. 73-84 (doi: 10.1016/j.compositesb.2015.10.032).

[2] L.A. Burns, A.P. Mouritz, D. Pook and S. Feih, Strength improvement to composite T-joints under bending through bio-inspired design, *Composites Part A*, **43**, 2012, pp. 1971-1980 (doi: 10.1016/j.compositesa.2012.06.017).

[3] R.D. Cope and R.B. Pipes, Design of the composite spar-wingskin joint, *Composites*, **13**, 1982, pp. 47-53 (doi: 10.1016/0010-4361(82)90170-7).

[4] F. Dharmawan, R.S. Thomson, H. Li, I. Herszberg and E. Gellert, Geometry and damage effects in a composite marine T-joint, *Composite Structures*, **66**, 2004, pp. 181-187 (doi: 10.1016/j.compstruct.2004.04.036).

[5] H. Cui, Y. Li, S. Koussios and A. Beukers, Parametric evaluation on the curved part of composite T-joints based on numerical simulation, *Proceedings of the 27th International Congress of the Aeronautical Sciences (Eds. I. Grant), Nice, France, September 19-24, 2010,* Optimage Ltd., UK, 8.6ST, 2010, pp. 1-10.

[6] J.L.S. Murillo, G.C. Ganzenmüller, S. Heimbs and M. May, Design parameter study of a CFRP T-joint under overpressure conditions due to ballistic impact, *Proceedings of the 17th European Conference on Composite Materials, Munich, Germany, June 26-30, 2016,* Fraunhofer-Publica, Germany, 2016, pp. 26-30.

[7] R.S. Trask, S.R. Hallet, F.M.M. Helenon and M.R. Wisnom, Influence of process induced defects on the failure of composite T-joint specimens, *Composites Part A*, **43**, 2012, pp. 748-757 (doi: 10.1016/j.compositesa.2011.12.021).

[8] D.W. Radford and R.J. Diefendorf, Shape instabilities in composites resulting from laminate anisotropy, *Journal of Reinforced Plastics and Composites*, **12**, 1993, pp. 58-75 (doi: 10.1177/073168449301200104).